Hydrol. Earth Syst. Sci. Discuss., 12, 4595–4630, 2015
www.hydrol-earth-syst-sci-discuss.net/12/4595/2015/
doi:10.5194/hessd-12-4595-2015
© Author(s) 2015. CC Attribution 3.0 License.

Hydrology and Earth System Sciences Discussions
Open Access

This discussion paper is/has been under review for the journal Hydrology and Earth System Sciences (HESS). Please refer to the corresponding final paper in HESS if available.

A global approach to defining flood seasons

D. Lee[1], P. Ward[2], and P. Block[1]

[1]University of Wisconsin – Madison, Madison, Wisconsin, USA
[2]Institute for Environmental Studies (IVM), VU University Amsterdam, Amsterdam, the Netherlands

Received: 8 April 2015 – Accepted: 10 April 2015 – Published: 30 April 2015

Correspondence to: P. Block (paul.block@wisc.edu)

Published by Copernicus Publications on behalf of the European Geosciences Union.

Abstract

Globally, flood catastrophes lead all natural hazards in terms of impacts on society, causing billions of dollars of damages annually. While short-term flood warning systems are improving in number and sophistication, forecasting systems on the order of months to seasons are a rarity, yet may lead to further disaster preparedness. To lay the groundwork for prediction, dominant flood seasons must be adequately defined. A global approach is adopted here, using the PCR-GLOBWB model to define spatial and temporal characteristics of major flood seasons globally. The main flood season is identified using a volume-based threshold technique. In comparison with observations, 40 % (50 %) of locations at a station (sub-basin) scale have identical peak months and 81 % (89 %) are within 1 month, indicating strong agreement between model and observed flood seasons. Model defined flood seasons are additionally found to well represent actual flood records from the Dartmouth Flood Observatory, further substantiating the models ability to reproduce the appropriate flood season. Minor flood seasons are also defined for regions with bi-modal streamflow climatology. Properly defining flood seasons can lead to prediction through association of streamflow with local and large-scale hydroclimatic indicators, and eventual integration into early warning systems for informed advanced planning and management. This is especially attractive for regions with limited observations and/or little capacity to develop early warning flood systems.

1 Introduction

Flood catastrophes lead all natural hazards in terms of impacts on society (Doocy et al., 2013). For example, the EM-DAT database (Centre for Research on the Epidemiology of Disasters) reports that hydrologic disasters in 2013 accounted for 48 % of all natural disasters and 45 % of global disaster mortality (Guha-Sapir et al., 2014). This is partially attributable to large populations living in flood-prone areas, growing by as much as 114 % between 1970 and 2010 (UNISDR, 2011). Flood disasters also rank as one

HESSD
12, 4595–4630, 2015

of the most destructive natural hazards in terms of economic damage, causing billions of dollars of damage each year (Munich Re, 2012). These flood damages have risen starkly over the past half-century given the rapid increase in global exposure (Bouwer, 2011; UNISDR, 2011; Visser et al., 2014).

In some regions, flood early warning systems have helped reduce loss of lives and assets by integrating with emergency planning and preparedness, from local to national scales (Golnaraghi et al., 2009; Kundzewicz et al., 2014; Revilla-Romero et al., 2014). Such systems have played an important role in various international initiatives, including the “Hyogo Framework for Action 2005–2015” and the “European Commission’s Flood Action Programme” (Revilla-Romero et al., 2014). The need remains, however, for additional early warning systems to foster improved flood risk management. Typically, flood forecast systems emphasize the short-term scale (hours to days) to inform immediate warnings and actions. Some examples of organizations and institutes having developed global early warning systems that target both early detection and early forecasting include CEOS (2014), GDACS (2014), GloFAS (2014), International Charter (2014), UNOSAT (2014) and the Dartmouth Flood Observatory (http://floodobservatory.colorado.edu/) (Alfieri et al., 2013; Revilla-Romero et al., 2014; Wu et al., 2012). Longer-range forecasts, on the order of months to seasons, however, can compliment short-range forecasts by focusing on disaster preparedness. For example, the International Federation of the Red Cross (IFRC) has been one of very few organizations to act on a long-range flood forecasts. In 2008, the IFRC implemented an early warning/early action strategy by mobilizing resources into the Niger River basin in West Africa in response to flood predictions. A flood did occur, and as a result of preparedness, relief supplies reached flood victims within days instead of weeks, preventing further loss of life and damages to livelihoods (Braman et al., 2013). Longer-range seasonal forecasts of streamflow also provide prospects for guiding water managers and basin organizations in decision-making beyond floods, including operation of water resources infrastructure, allocations, water trades, policy, regulation, and emergency

CC BY

response (Chiew et al., 2003; van Dijk et al., 2013; Pappenberger et al., 2011; Ritchie et al., 2004; Sankarasubramanian and Lall, 2003).

Only a small number of studies have investigated the seasonal predictability of streamflow impacts at continental or global scales, with minimal focus on flood forecasts. For example, Bierkens and van Beek (2009) evaluate seasonal predictability of winter and summer streamflow across the European continent with predictions of the North Atlantic Oscillation (NAO) Index as a main hydro-climatic driver, van Dijk et al. (2013) compare theoretical and actual skill in bi-monthly streamflow forecasts using a global ensemble streamflow prediction (ESP) system for 6192 small catchments across the world. Ward et al. (2014a) have shown that there is a strong link between El Niño–Southern Oscillation (ENSO) and annual river floods; and that these relationships also lead to anomalies in flood risk (in terms of economic damage and affected population) between normal years and the El Niño or La Niña years (Ward et al., 2014b). However, whilst they demonstrate this strong relationship, they did not explicitly link this to seasonal predictability. Therefore, there is a need to expand analyses targeting long-range streamflow predictions at the global scale.

To specifically address large-scale (annual) flood prediction from a global perspective, understanding and identifying seasonal spatial and temporal patterns of global streamflow becomes increasingly important, linking to global and regional climate behavior. In regions with dominant flood seasons, this may be trivial, however many regions express no dominant flood season (e.g. perpetually wet or dry, bi-modal flood seasons, etc.). Parsing out the annual flood season – if one exists – lays the groundwork for season-ahead flood prediction through the association of dominant streamflow with local and large-scale hydroclimatic indicators, and eventual integration into early warning systems for informed advanced planning and management. This is especially attractive for regions with limited observations and or little capacity to develop early warning flood systems. In this paper, we present an approach to properly define flood seasons using a global water balance model at the sub-basin and grid scale. These

HESSD
12, 4595–4630, 2015

CC BY

modeled flood seasons are subsequently validated with streamflow observations and historic flood records.

2 Data description

2.1 Streamflow stations

Daily streamflow observations utilized in this study are from the Global Runoff Data Centre (GRDC, 2007). Only stations having at least 20 years of continuous daily streamflow data were used (691 stations; Fig. 1).

2.2 PCR-GLOBWB

In this study, we evaluate simulations of daily streamflow over the period 1958–2000 taken from Ward et al. (2013), carried out using PCR-GLOBWB (PCRaster GLOBal Water Balance), a global hydrological model with a $0.5^{\circ} \times 0.5^{\circ}$ resolution (Van Beek and Bierkens, 2009; Van Beek et al., 2011). Note that for the simulations used in this study, the maximum storage within the river channel is based on geomorphological laws that do not account for existing flood protection measures such as dikes and levees.

For the simulations used in this study, the PCR-GLOBWB model was forced with daily meteorological data from the WATCH (Water and Global Change) project (Weedon et al., 2011), namely precipitation, temperature, and global radiation data. These data are available at the same resolution as the hydrological model ($0.5^{\circ} \times 0.5^{\circ}$). The WATCH forcing data were originally derived from the ERA-40 reanalysis product (Uppala et al., 2005), and were subjected to a number of corrections, described in (Weedon et al., 2011).

HESSD
12, 4595–4630, 2015

3 Defining flood seasons

Here we define major flood seasons as the 3-month period most likely to contain the annual maximum flood. The central month is referred to as the Peak Month (PM) and the full 3-month period is referred to as the Flood Season (FS). This approach is performed for both observed (station) and simulated (model) streamflow to gauge performance.

3.1 Methodology for defining grid-cell scale flood seasons

In the last few decades, a number of studies have investigated the timing of floods in the context of analyzing seasonality, frequency and trends. Generally, two main factors are emphasized regarding flood timing: streamflow volume and streamflow magnitude. For streamflow volume an occurrence date is commonly recorded, often in the context of trend analysis. For examples, Hodgkins and Dudley (2006) use winter-spring center of volume (WSCV) dates to analyze trends in snowmelt-induced floods, and Burn (2008) uses percentile of annual streamflow volume dates as indicators of flood timing, also for trend analysis. The second factor (streamflow magnitude) is traditionally more focused on peak-flood timing. Two sampling methods are frequently applied in hydrology. The first and most common is the annual-maximum (AM) method, which samples the largest streamflow in each year. The second method is the peaks-over-threshold (POT) method, first introduced by Smith (1984, 1987), in which all distinct, independent dominant peak flows greater than a fixed threshold are counted, prior to a specified date. In contrast to the AM method, the POT method can record multiple large independent floods within a year, including the annual maximum flow, but it can also miss the annual maximum flow in years in which streamflow is less than the threshold (Cunderlik and Ouarda, 2009; Cunderlik et al., 2004a; Ouarda et al., 1993). Thus, deciding the proper threshold for the POT method is important. Additionally, the POT method performs well under significant bi- or multi-modal flood conditions, and is typically more reliable than AM (e.g. see Cunderlik et al., 2004a).

HESSD
12, 4595–4630, 2015

CC BY

Therefore, to define the FS, and specifically the PM, globally, both volume and magnitude aspects need to be considered (Javelle et al., 2003). To do this, we adopt a volume-based threshold technique. This technique applies a prescribed streamflow volume threshold to identify flood occurrences. Here we select streamflow surpassing the top 5 % of the flow duration curve (FDC) across all years (1958–2000) as the threshold for considering a high streamflow level, as commonly adopted in threshold approaches (Burn, 2008; Mishra et al., 2011). The month containing the greatest number of days in the top 5 % is subsequently defined as the PM. Figure 2 provides an example based on seven years of synthetic streamflow; the number of days surpassing the 5 % threshold is listed for each month. In this example, August has the largest number of days over the threshold (105 days), thus August is defined as PM and July–September is defined as FS.

To evaluate the defined FS, we develop a simple evaluating statistic called the Percentage of Annual Maximum Flow (P_{AMF}). P_{AMF} is computed as shown in Eq. (1):

$$P_{\mathrm{AMF}} = \frac{n\mathrm{AMF}_{\mathrm{FS}}}{n\mathrm{AMF}_{\mathrm{total}}} \tag{1}$$

where $nAMF_{\mathrm{FS}}$ is the number of annual maximum flows that occurs in the FS (3-month) and $nAMF_{\mathrm{total}}$ is the total number of years. Thus, the P_{AMF} provides the percent of time the annual maximum flows occurs in the defined FS across the evaluation period. The P_{AMF} is relatively simple, yet inherently contains magnitude and volume properties of streamflow. For example, a high P_{AMF} indicates that the FS is highly likely to contain the annual maximum flood each year. In contrast, a low P_{AMF} indicates that the timing of the annual maximum flood is more likely to vary temporally, and may be a result of bimodal seasonality, consistently high or low streamflow throughout the year, or streamflow regulated by infrastructure. The P_{AMF} is calculated for both the observed streamflow at the selected 691 GRDC stations and the simulated streamflow at the associated 691 grid locations.

CC BY

3.2 Classification techniques

Clearly the volume-based threshold method is not the only available classification technique for defining the PM. To gauge its performance, the AM method and other volume methods with different given durations are selected for comparison, namely Q_{AM}, $Q_{7\,\text{day}}$, $Q_{15\,\text{day}}$ and $Q_{30\,\text{day}}$. For the Q_{AM} approach, which is based on the AM method, the FS is simply centered on the PM containing the largest number of annual maximum flow occurrences across the total years available. The $Q_{7\,\text{day}}$ approach defines the PM as the month with maximum streamflow volume during any seven consecutive day period; the month with the most periods across all years becomes the PM for the defined FS. The $Q_{15\,\text{day}}$ and $Q_{30\,\text{day}}$ approaches are similar to the $Q_{7\,\text{day}}$ approach, respectively using 15 and 30 days consecutively. The flow-based classification techniques with a shorter time component (1–7 days) favor identifying flood magnitude while the techniques with longer time components (15–30 days) favor identifying flood volume. The volume-based threshold method is an attempt to bridge these two criteria.

Cross-correlations of PM between the volume-based threshold technique and other classification techniques are quite high (0.87–0.90; Table 1), preliminarily indicating some success in capturing both magnitude and volume. The P_{AMF} is also useful for comparing classification techniques at stations and associated grid cells for which the selected PMs differ for at least one of the techniques. This occurs at 45 % of observed stations and 40 % of associated grid cells. The classification technique having the highest P_{AMF} most often for these stations and cells may be considered slightly superior. For model-based outputs, the volume-based threshold technique has the highest P_{AMF} by at least 2 %. Finally, classification technique performance may be evaluated by comparing the temporal difference (number of months) between model-based and observed PMs; closer is clearly superior. Overall the threshold technique produces a greater degree of similarity between model-based and observed PMs (2–5 % higher in ±1 month difference and 1–5 % higher in ±2 month difference). Based on these findings, the re-

CC BY

mainder of the analysis is carried out utilizing the volume-based threshold technique only.

3.3 Methodology for defining sub-basin scale flood seasons

In addition to evaluating the FS at the 691 grid cells based on model outputs, the FS is also defined at the sub-basin scale globally where observations are present. Previous studies have investigated flood seasonality as it relates to basin characteristics; for example, basins are often delineated and grouped according to similar flood seasonality (Burn, 1997; Cunderlik and Burn, 2002b; Cunderlik et al., 2004a; Ouarda et al., 1993), or conversely, flood seasonality is occasionally used to assess hydrological homogeneity of a group of regions (Cunderlik and Burn, 2002a; Cunderlik et al., 2004b), thus evaluating at the sub-basin scale is warranted.

While defining a single FS for a large-scale basin may be convenient, it may be difficult to justify given the potentially long travel times and varying climate, topography, vegetation, etc. Additionally, infrastructure may be present to regulate flow for flood control, water supply, irrigation, recreation, navigation, and hydropower (WCD, 2000), causing managed and natural flow regimes to differ drastically. This becomes important, as globally more than 33 000 records of large dams and reservoirs are listed (ICOLD, 1998–2009), with geo-referencing available for 6862 of them (Lehner et al., 2011). Nearly 50 % of large rivers with average streamflow in excess of $1000\,m^3\,s^{-1}$ are significantly modulated by dams (Lehner et al., 2011), often significantly attenuating flow hydrographs and flood volumes. The P_{AMF}, as previously defined, can aid in identifying stations downstream of a managed dam and reservoir.

To define a sub-basin's FS, the maximum P_{AMF} and associated PM for each station within the sub-basin are considered according to the following:

- If multiple stations exist within the sub-basin, the PM is defined as the PM occurring for the largest number of stations.

HESSD
12, 4595–4630, 2015

CC BY

- If there is a tie between months, their average P_{AMF} values are compared, and the month having the higher average P_{AMF} is defined as the PM.

- If there is a tie between months and equivalent average P_{AMF} values, the month having the higher average annual streamflow is defined as the PM.

This procedure is applied for both stations (observations) and corresponding grid cells (model) in each sub-basin. To illustrate, consider the 6 GRDC stations in the Zambezi River Basin (Fig. 3). For most of the stations, the observed PM is defined as a month later than the model-based PM (Table 2), an apparent bias in the model. The P_{AMF} of STA06 observations is noticeably lower than for other stations (36 %; Table 2) given its location downstream of the Itezhi-Tezhi dam (STA05) (Fig. 3). Otherwise, P_{AMF} values are consistently high across all stations. March is the PM identified most often, thus the final sub-basin PM selected is March.

In contrast, the model-based simulated streamflow produces a high P_{AMF} at STA06 (97 %), as the Itezhi-Tezhi dam is not represented in the simulations used for this study, and subsequently does not account for modulated streamflow. Across other stations, the P_{AMF} is also high, however an equal number of stations select February and March. In this case, February is selected as the final basin PM given its higher average P_{AMF} value (96 vs. 91 %).

By this approach, all 691 GRDC stations are grouped into 223 sub-basins to define the PM (Fig. 6); 58 % of sub-basins are defined by a single station, only 7.6 % (observations) and 8.1 % (model) of sub-basins have ties when defining PMs, and only one sub-basin has a tie between PMs and average P_{AMF} values.

4 Verification of selected flood seasons

Model-based FSs are verified by comparing with station observations and also flood records from the Dartmouth Flood Observatory (DFO).

HESSD
12, 4595–4630, 2015

4.1 Observed vs. modeled flood seasons

Ideally the model-based and observed GRDC stations have fully or partially overlapping FS periods. If so, this builds confidence in interpreting FSs at locations where no observed data are available. For comparing modeled FSs to observations, the defined PMs and calculated P_{AMF} are represented globally at the station scale (Figs. 4 and 5) and sub-basin scale (Fig. 6). Temporal differences are also compared (Figs. 7 and 8). For example, in the United States and Canada, 62 % of stations and 44 % of sub-basins produce identical PMs, growing to 82 % of stations and 96 % of sub-basins when considering a ±1 month temporal difference (Fig. 8). GRDC stations in the southeastern United States express relatively lower P_{AMF} values for observations (40–60 %) than model outputs (60–80 %), due to the high level of managed infrastructure. In the central United States and Europe, low P_{AMF} values are computed for both observation and model outputs (Fig. 5) with notable temporal differences in (Fig. 7). This is attributable, at least in part, to reservoirs and dams along the Mississippi, Missouri and Danube rivers.

Globally, comparing model and GRDC data, 40 % of the locations share the same 3 month FS. Considering a difference of ±1 month, this jumps to 81 and 91 % for ±2 months (Fig. 8). From a sub-basin perspective, the similarities are even stronger (50 % identical FS, 88 % ±1 month and 92 % ±2 month), indicating a relatively high level of agreement. For locations having dissimilar FSs (≥ ±3 months, 9 % of locations and 8 % of sub-basins), a substantial portion are located downstream of reservoirs directly, such as STA06 in the Zambezi example (Table 1), or are low-flow (dry) locations, both producing exceedingly low P_{AMF} values. Differences in FSs are not unexpected for low-flow locations, given the propensity for the annual streamflow maximum to potentially occur in a wide number of months. Overall, however, it appears that the global water balance model performs appropriately well in defining flood seasons globally at locations where observations are available.

HESSD

12, 4595–4630, 2015

CC BY

This may be subsequently extended to defining FSs and P_{AMF} at all grid cells (Figs. 9 and 10). Generally, a low P_{AMF} indicates an unstable FS, which occurs in cases of constant-flow, low-flow, bi-modal flow and regulated flow. All cases, except regulated flow, are simulated within the PCR-GLOBWB simulations used, thus the cell-based P_{AMF} values (Fig. 10) can provide a sense of confidence for the defined FS (Fig. 9). Examples of low-flow regions include the central United States and Australia; Europe exemplifies a constant-flow region, having low P_{AMF} regional values (Fig. 10). Bi-modal regions, such as much of East Africa with its two rainy seasons, may also be associated with low P_{AMF} values.

4.2 Modeled flood seasons vs. actual flood records

Model-based FSs may also be verified (subjectively) by surveying historic flood records. One such source is the Dartmouth Flood Observatory (DFO), a large, publically accessible repository of major flood events globally over 1985–2008, based on media and governmental reports and instrumental and remote sensing sources. Delineations of affected areas are best estimates (Brakenridge, 2011). The DFO records provide duration of each flooding event, as defined by the report or source, and represented as occurrence month (Fig. 11). DFO flood events and grid cell based PMs (Fig. 9) may be compared outright, however their characteristics differ slightly. The DFO covers 1985–2008 while the model represents 1958–2000. Also, the model-based PM represents the month most likely for a flood to occur; the DFO is simply a reporting of when the event did occur, regardless of whether it fell in the expected flood season or not. Nevertheless, model-based PMs and historic flooding records illustrate a striking similarity (compare Figs. 9 and 11), further supporting the model's ability to appropriately identify the PM spatially. Consistently, regions with high model-based P_{AMF} (80–100 %), such as Eastern South America, Central Africa and Central Asia, tend to agree well with DFO records, while low P_{AMF} (0–40 %) regions, such as Central North America, Europe, and East Africa, tend not to be in agreement with DFO records. In these low P_{AMF} regions, however, DFO records also illustrate floods occurring sporadi-

HESSD
12, 4595–4630, 2015

CC BY

cally throughout the year, further supporting accordance between cell-based P_{AMF} and DFO records (Figs. 10 and 11).

5 Defining minor flood seasons

In some climatic regions, there is no one single, well-defined flood season. For example, East Africa has two rainy seasons, the major season from June to September and the minor season from January to April/May. These two seasons are induced by northward and southward shifts of the inter-tropical convergence zone (Awange et al., 2014; Block and Strzepek, 2012; Chukalla et al., 2012; Romilly and Gebremichael, 2011; Segele et al., 2009a, b; Seleshi and Zanke, 2004). This bi-modal East African pattern allows for potential flooding in either season. In Canada, as another example, the dominant spring snowmelt season (March–May) and fall rainy season (August–October) allow for flood occurrences in either period (Cunderlik and Ouarda, 2009).

Previous studies have investigated techniques to differentiate seasonality from uni-, bi- and multi-modal streamflow climatologies and evaluate trends in timing and magnitude of streamflow, including the POT method, directional statistics method, and relative flood frequency method (Cunderlik and Ouarda, 2009; Cunderlik et al., 2004a). These methods may perform well at the local (case-specific) scale to define minor flood seasons, however applying them uniformly at the global scale can be problematic, given spatial heterogeneity. Additionally, even though bimodal streamflow climatology may be detected, the magnitude of streamflow in the minor season may or may not be negligible in regards to flooding potential as compared with the major season.

To detect noteworthy minor flood seasons, we classify streamflow regimes by climatology and monthly P_{AMF} value, which is the seasonal frequency of annual maximum flows (Fig. 12). Classifications include unimodal, bimodal, constant, and low-flow. The unimodal streamflow climatology has high values of P_{AMF} around the PM; the bimodal classification is represented by two peaks of P_{AMF}; both constant and low-flow classifications represent low values of P_{AMF} between months. Distinguishing between

Discussion Paper | Discussion Paper | Discussion Paper | Discussion Paper |

HESSD

12, 4595–4630, 2015

A global approach to defining flood seasons

D. Lee et al.

CC BY

bi-modal and other classifications is nontrivial. For example, upon initial inspection of the constant streamflow classification (both climatology and monthly P_{AMF}, Fig. 12c), it could be mistaken for a non-dominant bi-modal distribution. In other words, bi-modal streamflow could be detected correctly or incorrectly, depending on how to define bi-modal streamflow. We adopt the following criteria to differentiate bi-modal streamflow from uni-modal, constant and low-flow conditions.

- The low-flow classification is defined for annual average streamflow less than 1 cms.
- The major and minor PMs must be separated by at least two months in order to prevent an overlap of each FS (3-month).
- If the sum of both major and minor FS's P_{AMF} is greater than 80 % (minimum of 35 out of 43 annual maximums fall in one of the FS), it is defined as bi-modal streamflow.

After defining the major FS globally, the minor FS is identified if it matches the specified conditions. As previously mentioned, East Africa is a notable example of bi-modal streamflow, with evidence of floods in both the major and minor seasons (Fig. 13).

6 Conclusions and discussion

In this study, a global approach to define flood seasons is proposed to identify seasonal spatial and temporal patterns of global streamflow. Simulations of daily streamflow from the PCR-GLOBWB model are evaluated to define the dominant and minor flood seasons globally. In order to consider both streamflow magnitude and volume characteristics of floods, a volume-based threshold technique is applied to define the flood season and subsequently evaluated by the P_{AMF}. To verify model defined flood seasons, we compare with observations at both station and sub-basin scales. As a result, 40 % (50 %) of locations at the station (sub-basin) scale have identical peak months and 81 %

(89 %) are within 1 month, indicating strong agreement between model and observed flood seasons. Model defined flood seasons are additionally found to well represent actual flood records from the Dartmouth Flood Observatory, further substantiating the models ability to reproduce the appropriate flood season. Regions expressing bi-modal streamflow climatology are also defined to illustrate potential for noteworthy secondary flood seasons.

Identifying major flood seasons globally has numerous advantages, including improved understanding of flood potential, causation, and management, particularly in ungauged or limited-gauged basins, potentially leading to development of season-ahead flood warning systems. Another advantage, and main motivation behind this work, is to lay the groundwork for season-ahead flood prediction through the association of dominant streamflow with local and large-scale hydroclimatic indicators. Information at this scale can be complimentary to short-term flood predictions, motivating governments and relief agencies to plan and mobilize resources accordingly to minimize flood impacts on lives and livelihoods.

Outcomes of this work also link global and regional climate behavior with seasonal spatial and temporal patterns of streamflow. For example, global monsoon systems are clearly evident, as driven by the ITCZ, in central and southern Africa, Asia and northern South America (Fig. 9). Latitudinal patterns in the extra-tropics are also quite distinct, with flood seasons often occurring across similar months in the year. The fingerprints of regional climate systems influencing flood seasons are also prevalent, including the North American monsoon and South Atlantic Convergence Zone. In some cases non-adjacent regions express similar flood seasons and characteristics, indicating similar influence by large-scale climate dynamics, ENSO being the best understood; regions of similarity and their associated climate dynamics warrant further attention.

Defining major flood seasons and the climate precursors leading to those seasons offer strong prospects for developing season-ahead flood prediction models. To examine seasonal predictability of annual floods globally, the co-variability between streamflow and global and regional climatic indicators will be identified and related through em-

HESSD
12, 4595–4630, 2015

CC BY

pirical models to gauge predictive skill. Concurrently, basin-level tailored flood forecast models will be constructed at selected locations for comparing predictive capabilities with the global approach. While both scales play an important part, for basins in which the global approach is sufficiently skillful, it may serve as a useful tool for international disaster management, particularly in vulnerable un-gauged regions, without necessitating a data-heavy, physically-based, local model.

Acknowledgements. Philip Ward was funded by a VENI grant from the Netherlands Organisation for Scientific Research (NWO).

References

Alfieri, L., Burek, P., Dutra, E., Krzeminski, B., Muraro, D., Thielen, J., and Pappenberger, F.: GloFAS – global ensemble streamflow forecasting and flood early warning, Hydrol. Earth Syst. Sci., 17, 1161–1175, doi:10.5194/hess-17-1161-2013, 2013.

Awange, J. L., Gebremichael, M., Forootan, E., Wakbulcho, G., Anyah, R., Ferreira, V. G., and Alemayehu, T.: Characterization of Ethiopian mega hydrogeological regimes using GRACE, TRMM and GLDAS datasets, Adv. Water Resour., 74, 64–78, doi:10.1016/j.advwatres.2014.07.012, 2014.

Bierkens, M. F. P. and van Beek, L. P. H.: Seasonal predictability of European discharge: NAO and hydrological response time, J. Hydrometeorol., 10, 953–968, doi:10.1175/2009JHM1034.1, 2009.

Block, P. and Strzepek, K.: Power ahead: meeting Ethiopia's energy needs under a changing climate, Rev. Dev. Econ., 16, 476–488, doi:10.1111/j.1467-9361.2012.00675.x, 2012.

Bouwer, L. M.: Have disaster losses increased due to anthropogenic climate change?, B. Am. Meteorol. Soc., 92, 39–46, doi:10.1175/2010BAMS3092.1, 2011.

Brakenridge, G. R.: Global Active Archive of Large Flood Events, Dartmouth Flood Observatory, University of Colorado, available from: http://floodobservatory.colorado.edu/Archives/index.html (last access: 27 April 2015), 2011.

Braman, L. M., van Aalst, M. K., Mason, S. J., Suarez, P., Ait-Chellouche, Y., and Tall, A.: Climate forecasts in disaster management: red Cross flood operations in West Africa, 2008, Disasters, 37, 144–64, doi:10.1111/j.1467-7717.2012.01297.x, 2013.

CC BY

Burn, D. H.: Catchment similarity for regional flood frequency analysis using seasonality measures, J. Hydrol., 202, 212–230, doi:10.1016/S0022-1694(97)00068-1, 1997.
Burn, D. H.: Climatic influences on streamflow timing in the headwaters of the Mackenzie River Basin, J. Hydrol., 352, 225–238, doi:10.1016/j.jhydrol.2008.01.019, 2008.
CEOS: Committee on Earth Observation Satellites (CEOS) Flood Pilot, available at: http://ceos.org/ourwork/workinggroups/disasters/floods/ (last access: 27 April 2015), 2014.
Chiew, F. H. S., Zhou, S. L., and McMahon, T. A.: Use of seasonal streamflow forecasts in water resources management, J. Hydrol., 270, 135–144, doi:10.1016/S0022-1694(02)00292-5, 2003.
Chukalla, A. D., Haile, A. M., and Schultz, B.: Optimum irrigation and pond operation to move away from exclusively rainfed agriculture: the Boru Dodota Spate Irrigation Scheme, Ethiopia, Irrig. Sci., 31, 1091–1102, doi:10.1007/s00271-012-0390-9, 2012.
Cunderlik, J. M. and Burn, D. H.: Local and regional trends in monthly maximum flows in Southern British Columbia, Can. Water Resour. J., 27, 191–212, doi:10.4296/cwrj2702191, 2002a.
Cunderlik, J. M. and Burn, D. H.: The use of flood regime information in regional flood frequency analysis, Hydrol. Sci. J., 47, 77–92, doi:10.1080/02626660209492909, 2002b.
Cunderlik, J. M. and Ouarda, T. B. M. J.: Trends in the timing and magnitude of floods in Canada, J. Hydrol., 375, 471–480, doi:10.1016/j.jhydrol.2009.06.050, 2009.
Cunderlik, J. M., Ouarda, T. B. M. J., and Bobée, B.: Determination of flood seasonality from hydrological records/Détermination de la saisonnalité des crues à partir de séries hydrologiques, Hydrol. Sci. J., 49, 511–526, doi:10.1623/hysj.49.3.511.54351, 2004a.
Cunderlik, J. M., Ouarda, T. B. M. J., and Bobée, B.: On the objective identification of flood seasons, Water Resour. Res., 40, W01520, doi:10.1029/2003WR002295, 2004b.
Döll, P. and Lehner, B.: Validation of a new global 30-min drainage direction map, J. Hydrol., 258, 214–231, doi:10.1016/S0022-1694(01)00565-0, 2002.
Doocy, S., Daniels, A., Murray, S., and Kirsch, T. D.: The human impact of floods: a historical review of events 1980–2009 and systematic literature review., PLoS Curr., 5, 1–27, doi:10.1371/currents.dis.f4deb457904936b07c09daa98ee8171a, 2013.
GDACS: Global Disaster Alert and Coordination System, available at: http://www.gdacs.org/ (last access: 27 April 2015), 2014.
Global Runoff Data Centre: Major River Basins of the World/Global Runoff Data Centre, Federal Institute of Hydrology (BfG), Koblenz, Germany, available at: http://www.bafg.de/GRDC/EN/Home/homepage_node.html (last access: 27 April 2015), 2007.

HESSD
12, 4595–4630, 2015

A global approach to defining flood seasons

D. Lee et al.

CC BY

GloFAS: Global Flood Awareness System, available at: http://www.globalfloods.eu/en/ (last access: 27 April 2015), 2014.
Golnaraghi, M., Douris, J., and Migraine, J.-B.: Saving Lives Through Early Warning Systems and Emergency Preparedness, Risk Wise, Tudor Rose, 2009.
Guha-Sapir, D., Hoyois, P., and Below, R.: Annual Disaster Statistical Review 2013: The Numbers and Trends, CRED, Brussels, 2014.
Hodgkins, G. A. and Dudley, R. W.: Changes in the timing of winter-spring streamflows in eastern North America, 1913–2002, Geophys. Res. Lett., 33, 1–5, doi:10.1029/2005GL025593, 2006.
ICOLD (International Commission on Large Dams): World Register of Dams. Version updates 1998–2009, ICOLD, Paris, available at: www.icold-cigb.org (last access: 27 April 2015), 2009.
International Charter: on Space and Major Disasters, available at: https://www.disasterscharter.org (last access: 27 April 2015), 2014.
Javelle, P., Ouarda, T. B. M. J., and Bobée, B.: Spring flood analysis using the flood-duration-frequency approach: application to the provinces of Quebec and Ontario, Canada, Hydrol. Process., 17, 3717–3736, doi:10.1002/hyp.1349, 2003.
Kundzewicz, Z. W., Kanae, S., Seneviratne, S. I., Handmer, J., Nicholls, N., Peduzzi, P., Mechler, R., Bouwer, L. M., Arnell, N., Mach, K., Muir-Wood, R., Brakenridge, G. R., Kron, W., Benito, G., Honda, Y., Takahashi, K., and Sherstyukov, B.: Flood risk and climate change: global and regional perspectives, Hydrolog. Sci. J., 59, 1–28, doi:10.1080/02626667.2013.857411, 2014.
Lehner, B., Liermann, C. R., Revenga, C., Vörösmarty, C., Fekete, B., Crouzet, P., Döll, P., Endejan, M., Frenken, K., Magome, J., Nilsson, C., Robertson, J. C., Rödel, R., Sindorf, N., and Wisser, D.: High-resolution mapping of the world's reservoirs and dams for sustainable river-flow management, Front. Ecol. Environ., 9, 494–502, doi:10.1890/100125, 2011.
Mishra, A. K., Singh, V. P., and Özger, M.: Seasonal streamflow extremes in Texas river basins: uncertainty, trends, and teleconnections, J. Geophys. Res. Atmos., 116, 1–28, doi:10.1029/2010JD014597, 2011.
Munich Re: Topics Geo 2012 Issue. Natural Catastrophes 2011. Analyses, Assessments, Positions, Münchener Rückversicherungs-Gesellschaft, Munich, 2012.

CC BY

Ouarda, T. B. M. J., Ashkar, F., and El-Jabi, N.: Peaks over threshold model for seasonal flood variations, in: Engineering Hydrology: Proceedings of the Symposium, edited by: Kuo, C. Y., 341–346, Amerian Society of Civil Enngineers, Reston, VA, 1993.

Pappenberger, F., Thielen, J., and Del Medico, M.: The impact of weather forecast improvements on large scale hydrology: analysing a decade of forecasts of the European Flood Alert System, Hydrol. Process., 25, 1091–1113, doi:10.1002/hyp.7772, 2011.

Revilla-Romero, B., Thielen, J., Salamon, P., De Groeve, T., and Brakenridge, G. R.: Evaluation of the satellite-based Global Flood Detection System for measuring river discharge: influence of local factors, Hydrol. Earth Syst. Sci., 18, 4467–4484, doi:10.5194/hess-18-4467-2014, 2014.

Ritchie, J. W., Zammit, C., and Beal, D.: Can seasonal climate forecasting assist in catchment water management decision-making?, Agric. Ecosyst. Environ., 104, 553–565, doi:10.1016/j.agee.2004.01.029, 2004.

Romilly, T. G. and Gebremichael, M.: Evaluation of satellite rainfall estimates over Ethiopian river basins, Hydrol. Earth Syst. Sci., 15, 1505–1514, doi:10.5194/hess-15-1505-2011, 2011.

Sankarasubramanian, A. and Lall, U.: Flood quantiles in a changing climate: seasonal forecasts and causal relations, Water Resour. Res., 39, 1134, doi:10.1029/2002WR001593, 2003.

Segele, Z. T., Lamb, P. J., and Leslie, L. M.: Large-scale atmospheric circulation and global sea surface temperature associations with Horn of Africa June–September rainfall, Int. J. Climatol., 29, 1075–1100, doi:10.1002/joc.1751, 2009a.

Segele, Z. T., Lamb, P. J., and Leslie, L. M.: Seasonal-to-interannual variability of Ethiopia/Horn of Africa monsoon. Part I: Associations of wavelet-filtered large-scale atmospheric circulation and global sea surface temperature, J. Climate, 22, 3396–3421, doi:10.1175/2008JCLI2859.1, 2009b.

Seleshi, Y. and Zanke, U.: Recent changes in rainfall and rainy days in Ethiopia, Int. J. Climatol., 24, 973–983, doi:10.1002/joc.1052, 2004.

Smith, R. L.: Threshold methods for sample extremes, in: Statistical Extremes and Applications, D. Reidel, Dordrecht, the Netherlands, 621–638, 1984.

Smith, R. L.: Estimating tails of probability distributions, Ann. Stat., 15, 1174–1207, doi:10.1214/aos/1176350499, 1987.

HESSD

12, 4595–4630, 2015

A global approach to defining flood seasons

D. Lee et al.

UNISDR: Global Assessment Report on Disaster Risk Reduction (GAR 11) – Revealing Risk, Redefining Development, United Nations Office for Disaster Risk Reduction (UNISDR), Geneva, Switzerland, 2011.

UNISDR: Global Assessment Report on Disaster Risk Reduction (GAR 13) – From Shared Risk to Shared Value: The Business Case for Disaster Risk Reduction, United Nations Office for Disaster Risk Reduction (UNISDR), Geneva, Switzerland, 2013.

UNISDR: Global Assessment Report on Disaster Risk Reduction (GAR 15) – Making Development Sustainable: The Future of Disaster Risk Management, United Nations Office for Disaster Risk Reduction (UNISDR), Geneva, Switzerland, 2015.

UNOSAT: UNITAR Operational Satellite Applications Programme, available at: http://www.unitar.org/unosat/ (last access: 27 April 2015), 2014.

Uppala, S. M., KÅllberg, P. W., Simmons, A. J., Andrae, U., Bechtold, V. D. C., Fiorino, M., Gibson, J. K., Haseler, J., Hernandez, A., Kelly, G. A., Li, X., Onogi, K., Saarinen, S., Sokka, N., Allan, R. P., Andersson, E., Arpe, K., Balmaseda, M. A., Beljaars, A. C. M., Berg, L. Van De, Bidlot, J., Bormann, N., Caires, S., Chevallier, F., Dethof, A., Dragosavac, M., Fisher, M., Fuentes, M., Hagemann, S., Hólm, E., Hoskins, B. J., Isaksen, L., Janssen, P. A. E. M., Jenne, R., Mcnally, A. P., Mahfouf, J.-F., Morcrette, J.-J., Rayner, N. A., Saunders, R. W., Simon, P., Sterl, A., Trenberth, K. E., Untch, A., Vasiljevic, D., Viterbo, P., and Woollen, J.: The ERA-40 re-analysis, Q. J. Roy. Meteor. Soc., 131, 2961–3012, doi:10.1256/qj.04.176, 2005.

Van Beek, L. P. H. and Bierkens, M. F. P.: The Global Hydrological Model PCR-GLOBWB: Conceptualization, Parameterization and Verification, available at: http://vanbeek.geo.uu.nl/suppinfo/vanbeekbierkens2009.pdf (last access: 27 April 2015) Department of Physical Geography, Utrecht University, Utrecht, the Netherlands, 2009.

Van Beek, L. P. H., Wada, Y., and Bierkens, M. F. P.: Global monthly water stress: 1. Water balance and water availability, Water Resour. Res., 47, W07517, doi:10.1029/2010WR009791, 2011.

Van Dijk, A. I. J. M., Peña-Arancibia, J. L., Wood, E. F., Sheffield, J., and Beck, H. E.: Global analysis of seasonal streamflow predictability using an ensemble prediction system and observations from 6192 small catchments worldwide, Water Resour. Res., 49, 2729–2746, doi:10.1002/wrcr.20251, 2013.

Visser, H., Petersen, A. C., and Ligtvoet, W.: On the relation between weather-related disaster impacts, vulnerability and climate change, Clim. Change, 125, 461–477, doi:10.1007/s10584-014-1179-z, 2014.

Ward, P. J., Jongman, B., Weiland, F. S., Bouwman, A., van Beek, R., Bierkens, M. F. P., Ligtvoet, W., and Winsemius, H. C.: Assessing flood risk at the global scale: model setup, results, and sensitivity, Environ. Res. Lett., 8, 044019, doi:10.1088/1748-9326/8/4/044019, 2013.

Ward, P. J., Eisner, S., Flörke, M., Dettinger, M. D., and Kummu, M.: Annual flood sensitivities to El Niño–Southern Oscillation at the global scale, Hydrol. Earth Syst. Sci., 18, 47–66, doi:10.5194/hess-18-47-2014, 2014a.

Ward, P. J., Jongman, B., Kummu, M., Dettinger, M. D., Sperna Weiland, F. C., and Winsemius, H. C.: Strong influence of El Nino Southern Oscillation on flood risk around the world, P. Natl. Acad. Sci. USA, 111, 15659–15664, doi:10.1073/pnas.1409822111, 2014b.

WCD (World Commission on Dams): Dams and Development: a Framework For Decision Making, Earthscan, London, UK, 2000.

Weedon, G. P., Gomes, S., Viterbo, P., Shuttleworth, W. J., Blyth, E., Österle, H., Adam, J. C., Bellouin, N., Boucher, O., and Best, M.: Creation of the WATCH forcing data and its use to assess global and regional reference crop evaporation over land during the twentieth century, J. Hydrometeorol., 12, 823–848, doi:10.1175/2011JHM1369.1, 2011.

Wu, H., Adler, R. F., Hong, Y., Tian, Y., and Policelli, F.: Evaluation of global flood detection using satellite-based rainfall and a hydrologic model, J. Hydrometeorol., 13, 1268–1284, doi:10.1175/JHM-D-11-087.1, 2012.

HESSD
12, 4595–4630, 2015

A global approach to defining flood seasons

D. Lee et al.

Table 1. Cross-correlations of Peak Month (PM) at GRDC stations for each classification technique for **(a)** observed and **(b)** simulated streamflow.

Classification Technique		Threshold	Q_{AM}	$Q_{7\text{ day}}$	$Q_{15\text{ day}}$	$Q_{30\text{ day}}$
Observed	Threshold	1				
	Q_{AM}	0.866	1			
	$Q_{7\text{ day}}$	0.894	0.912	1		
	$Q_{15\text{ day}}$	0.895	0.880	0.945	1	
	$Q_{30\text{ day}}$	0.900	0.832	0.881	0.890	1
Simulated	Threshold	1				
	Q_{AM}	0.849	1			
	$Q_{7\text{ day}}$	0.873	0.926	1		
	$Q_{15\text{ day}}$	0.884	0.912	0.940	1	
	$Q_{30\text{ day}}$	0.888	0.880	0.902	0.911	1

HESSD
12, 4595–4630, 2015

HESSD
12, 4595–4630, 2015

A global approach to defining flood seasons

D. Lee et al.

CC BY

Table 2. Comparison of Peak Month (PM) for flooding and calculated P_{AMF} at 6 GRDC stations in the Zambezi River Basin.

Station (GRDC sta. numb.)	STA01 (1591001)		STA02 (1291100)		STA03 (1591406)		STA04 (1591404)		STA05 (1591403)		STA06 (1591401)		Final PM
Station name	Senanga		Katima Mulilo		Machiya Ferry		Kafue Hook Bridge		Itezhi-Tezhi		Kasaka		
River name	Zambezi		Zambezi		Kafue		Kafue		Kafue		Kafue		
Cumulative catchment area (km^2)	284 538		339 521		23 065		96 239		105 672		153 351		
Mean annual streamflow (m^3 s^{-1})	975		1168		139		287		353		988		
Streamflow type	Natural		Natural		Natural		Natural		Natural (Reservoir inflow)		Regulated		
Classification Technique	PM (month)	P_{AMF} (%)	PM (month)	P_{AMF} (%)	PM (month)	P_{AMF} (%)	PM (month)	P_{AMF} (%)	PM (month)	P_{AMF} (%)	PM (month)	P_{AMF} (%)	
Observed	4	96	4	100	3	93	3	100	3	94	7	36	3
Simulated	3	100	3	97	2	97	3	75	2	94	2	97	2

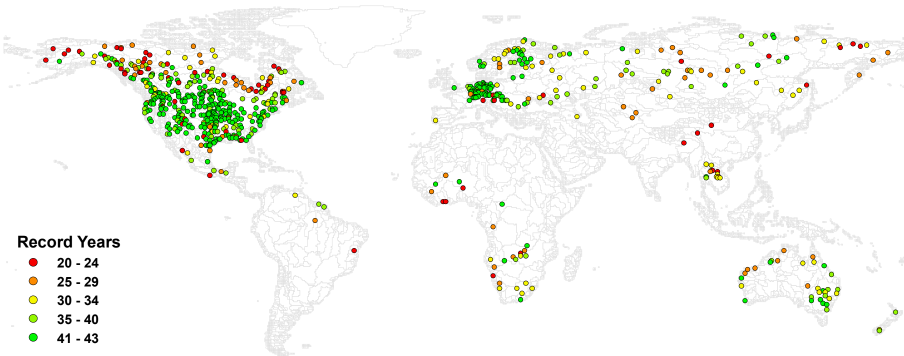

Figure 1. Location of 691 selected GRDC stations with corresponding number of years per station. Background polygons are world sub-basins based on 30′ drainage direction maps (Döll and Lehner, 2002).

HESSD
12, 4595–4630, 2015

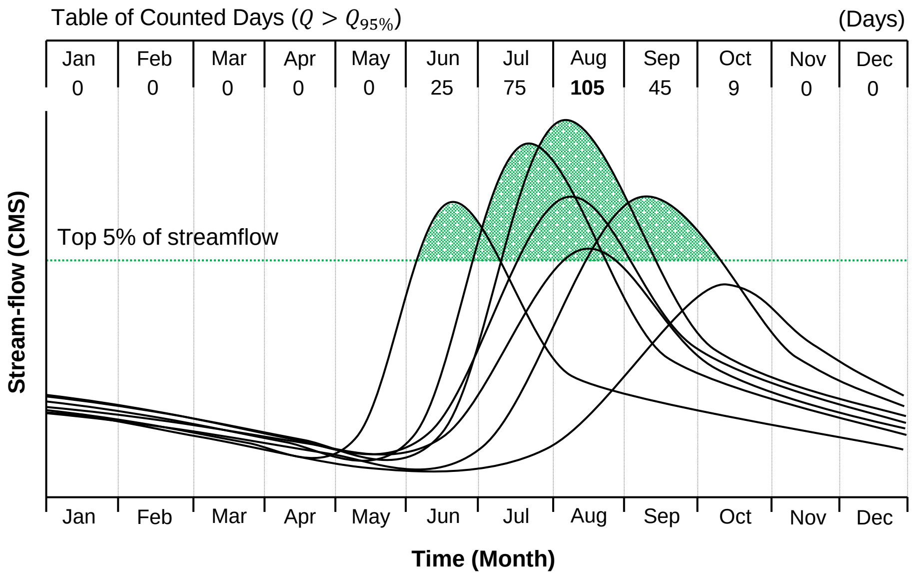

Figure 2. Seven years of synthetic streamflow data. Dotted line represents the 5 % streamflow threshold. Numbers indicates the total days above the threshold for each month.

HESSD
12, 4595–4630, 2015

A global approach to defining flood seasons

D. Lee et al.

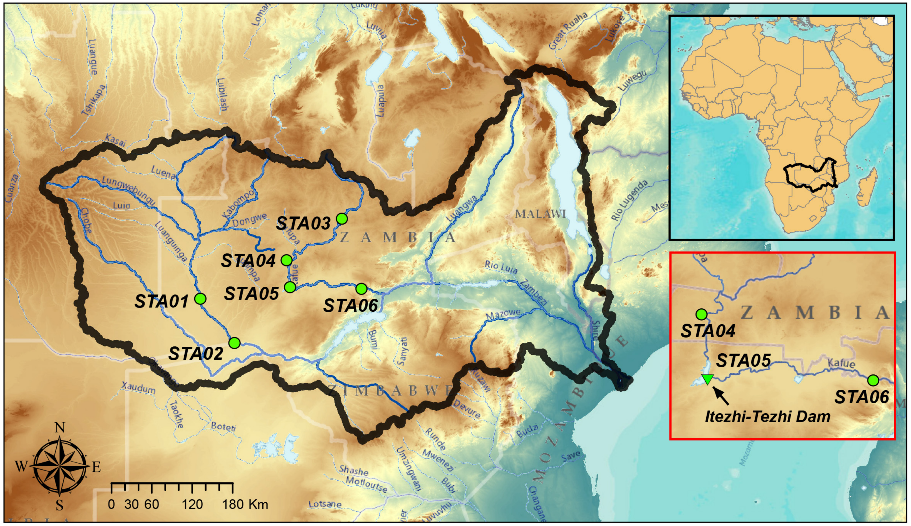

Figure 3. Map of Zambezi River Basin; the solid black line delineates the basin and the green points are the 6 GRDC stations (STA01-06), with STA06 downstream of the Itezhi-Tezhi dam (STA05).

CC BY

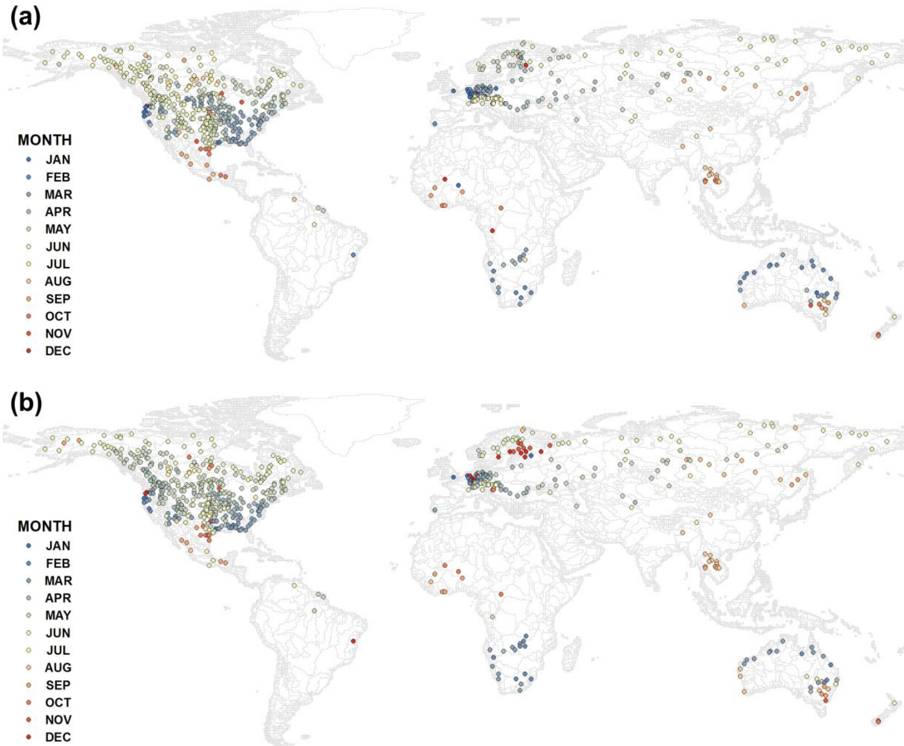

Figure 4. Peak Month (PM) for flooding as defined by **(a)** 691 GRDC observation stations, and **(b)** simulated streamflow at associated locations.

HESSD
12, 4595–4630, 2015

A global approach to defining flood seasons

D. Lee et al.

CC BY

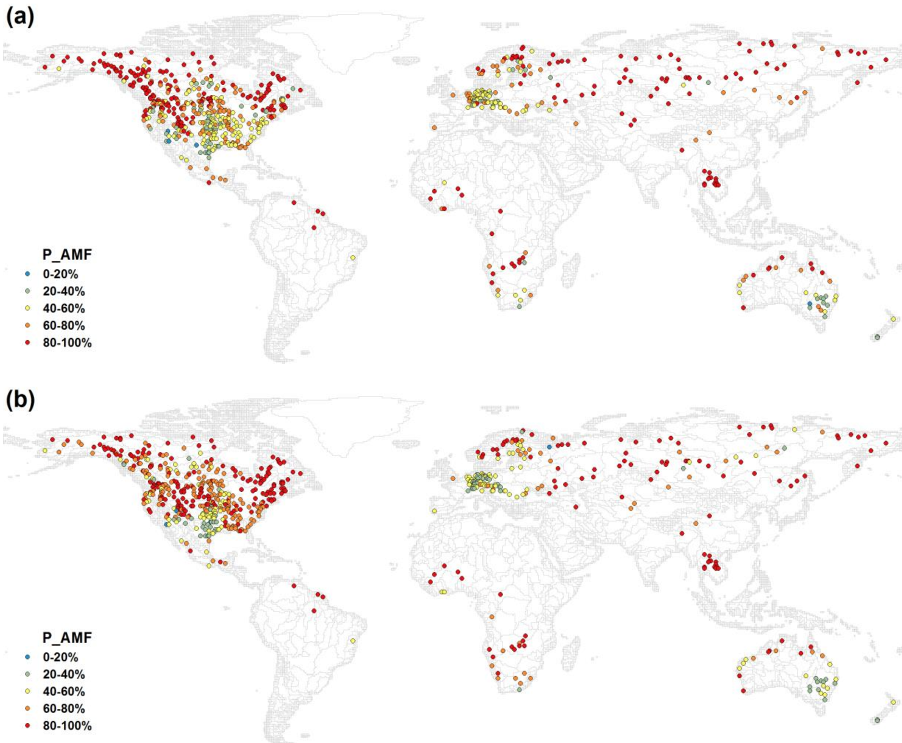

Figure 5. Calculated P_{AMF} values for **(a)** 691 GRDC observation stations, and **(b)** simulated streamflow.

HESSD
12, 4595–4630, 2015

A global approach to defining flood seasons

D. Lee et al.

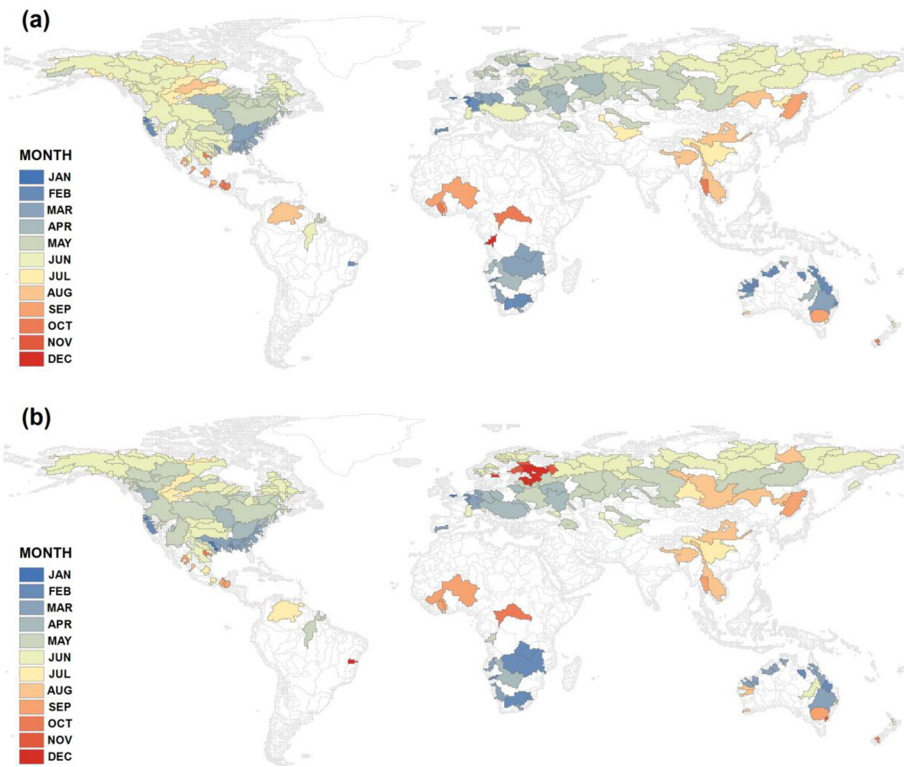

Figure 6. Peak Month (PM) for flooding by sub-basin as defined by **(a)** 691 GRDC observation stations, and **(b)** simulated streamflow at associated sub-basins.

HESSD
12, 4595–4630, 2015

CC BY

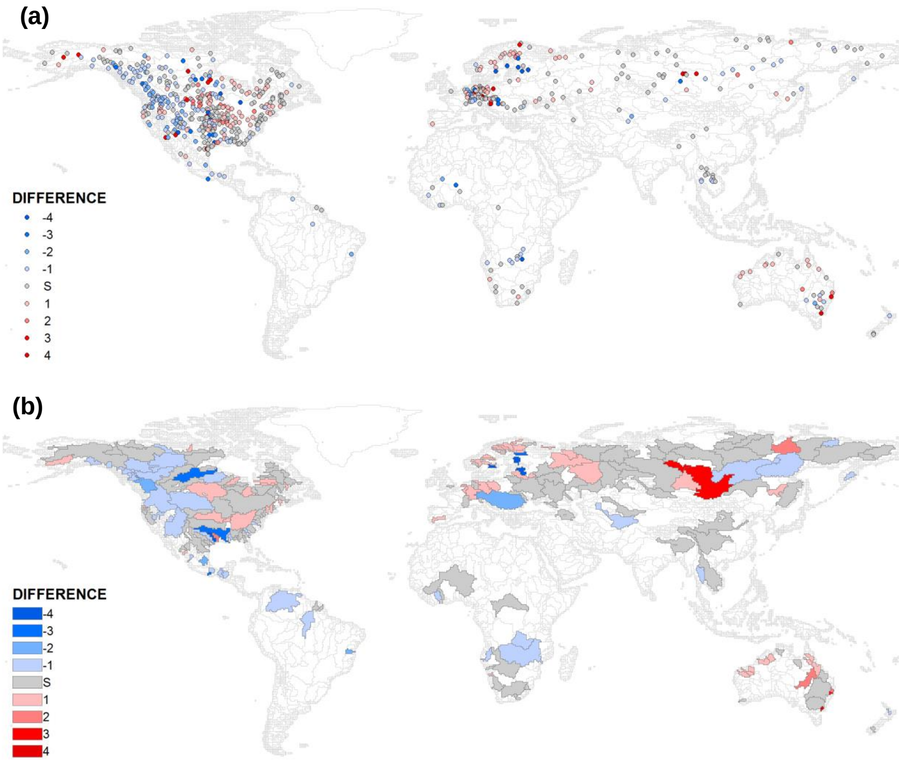

Figure 7. Temporal difference (number of months) in Flood Season (FS) between observations and model outputs by **(a)** station locations, and **(b)** sub-basins.

HESSD
12, 4595–4630, 2015

CC BY

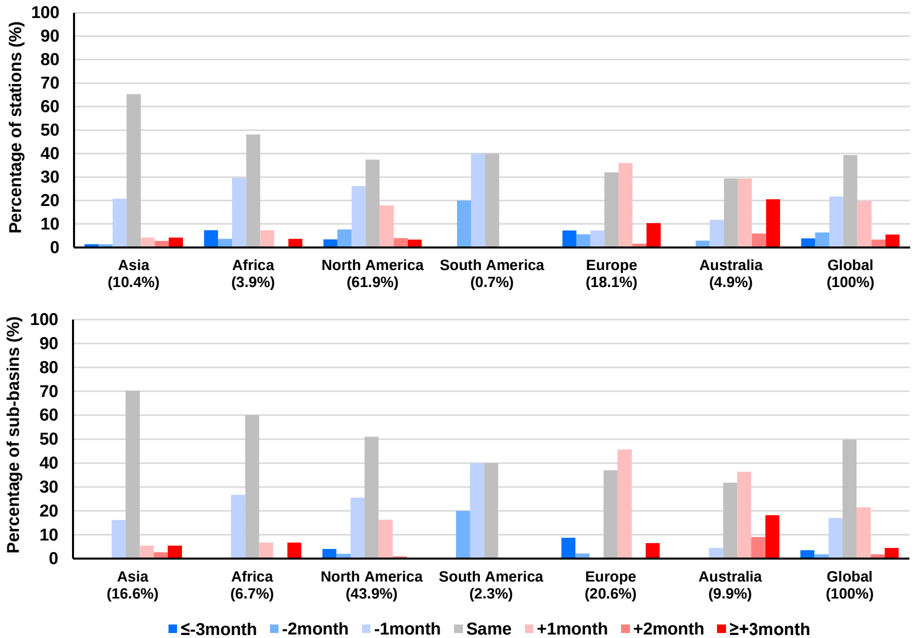

Figure 8. Percentage of stations (above) and sub-basins (below) according to temporal difference of FS between observations and model outputs in each continent.

HESSD
12, 4595–4630, 2015

CC BY

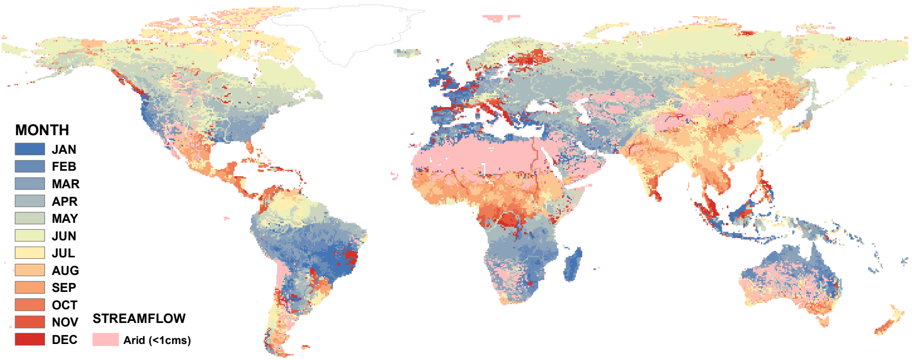

Figure 9. Peak Month (PM) for flooding as defined at all modeled grid cells.

HESSD
12, 4595–4630, 2015

A global approach to defining flood seasons

D. Lee et al.

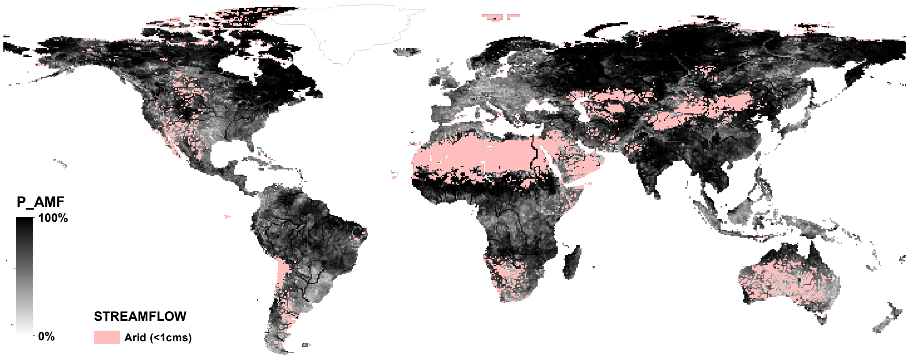

Figure 10. Calculated P_{AMF} values for at all modeled grid cells.

HESSD
12, 4595–4630, 2015

A global approach to defining flood seasons

D. Lee et al.

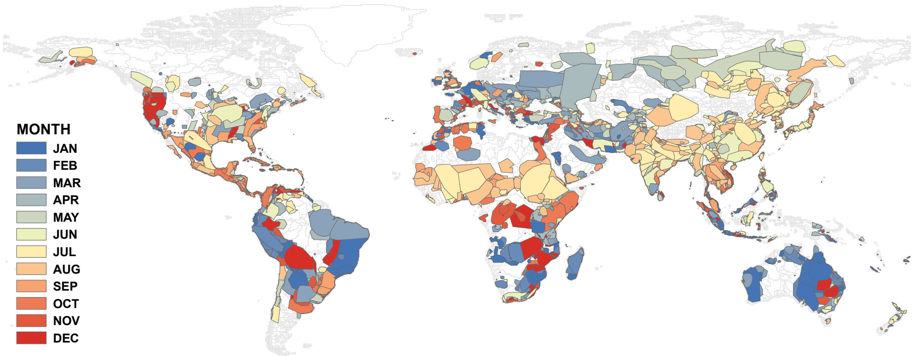

Figure 11. Archive of major flood events globally from the Dartmouth Flood Observatory (DFO) over 1985–2008.

HESSD
12, 4595–4630, 2015

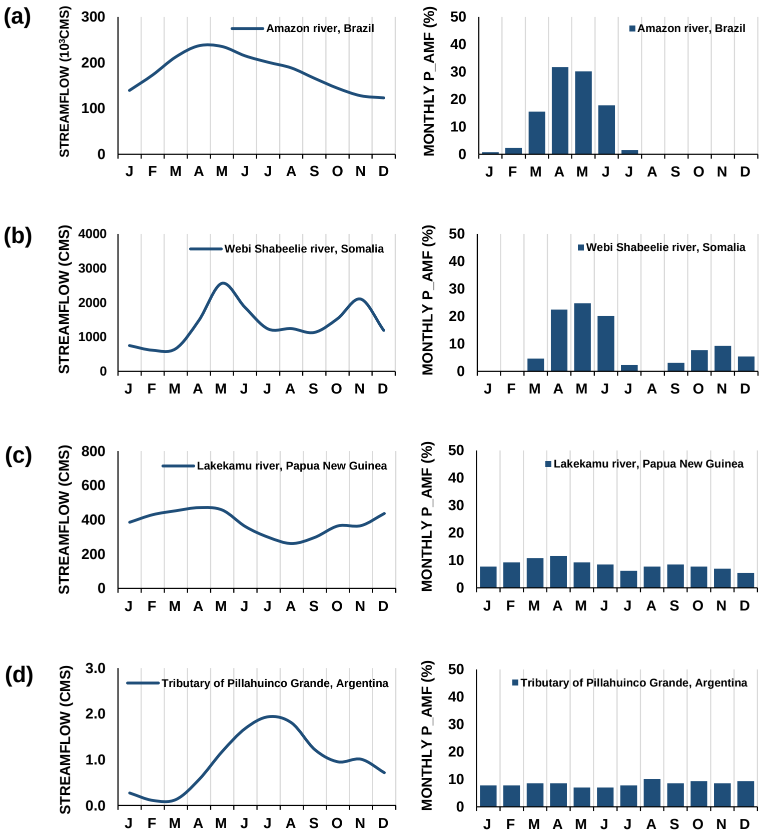

Figure 12. Model-based streamflow climatology (left) and corresponding monthly P_{AMF} (right). Types and locations are: **(a)** uni-modal streamflow – Amazon river, Brazil, **(b)** bimodal streamflow – Webi Shabeelie river, Somalia, **(c)** constant streamflow – Lakekamu river, Papua New Guinea and **(d)** low-flow – Tributary of Pillahuinco Grande, Argentina.

HESSD
12, 4595–4630, 2015

CC BY

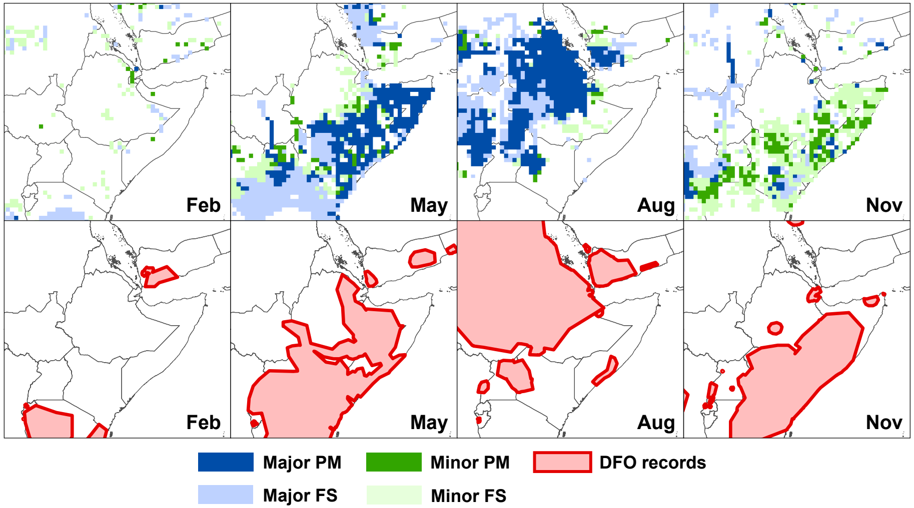

Figure 13. East Africa's monthly total flood seasons (above); peak month of major and minor flood seasons (dense color) and post-month of prior FS and pre-month of next FS (light color). Monthly accumulated actual flood records (DFO) during 1958–2008 (below).

HESSD
12, 4595–4630, 2015

A global approach to defining flood seasons

D. Lee et al.